

## A Highly Selective Fluorescence and Electrochemical Sensor for Ni(II) Ions based on 4-(4-phenylthiazole-2-ylimino)pent-2-en-2-ol

Vinod Kumar Gupta<sup>1,2,\*</sup>

<sup>1</sup>Department of Chemistry, Indian Institute of Technology Roorkee, Roorkee-247 667, India

<sup>2</sup>Department of Applied Chemistry, University of Johannesburg, Johannesburg, South Africa

\*E-mail: [vinodfcy@iitr.ac.in](mailto:vinodfcy@iitr.ac.in); [vinodfcy@gmail.com](mailto:vinodfcy@gmail.com)

Received: 11 July 2015 / Accepted: 5 August 2015 / Published: 12 August 2015

---

A new thiazole functionalized fluorogenic ionophore M1 was synthesized and characterized with NMR and IR spectroscopy. Fluorescence responses toward various metal ions were explored on photo-fluorescence spectroscopy. The sensor M1 exhibited high selective and sensitive electrochemical and fluorescence response to Ni<sup>2+</sup> in the existence of various competing metal ions with high value of association constant  $1.07 \times 10^4 \text{ M}^{-1}$ . These spectral changes are enough for naked-eye detection. The results revealed that the sensor provides reversible fluorescence strategy with EDTA.

---

**Keywords:** Chemosensor, Naked eye sensor, Reversibility, Electrochemical sensing, Nickel ion.

### 1. INTRODUCTION

Transition and heavy metal ions pose a vital task in the wide range of environmental and biological species, and the development of a more selective cation recognition system has received a great attention. Along with the other transition metal series, nickel is an essential trace element in biological systems, which are widely use in metallurgical processes namely alloy production with iron, electroplating and nickel–cadmium batteries [1-2]. Wide varieties of food such as chocolate, raw meat, milk and milk products, hydrogenated oils, and canned food, etc, are also contained low concentration of nickel ion. Moderately toxic natures of nickel ion are responsible for asthma, nasal and lung cancer, and central nervous system disorder [3–6]. Thus, it is needed to design Ni<sup>2+</sup> ion sensors that possess high selective and sensitive signalling mechanisms. Numerous analytical and sophisticated techniques such as inductively coupled plasma mass spectroscopy(ICP-MS), atomic absorption spectrometry(AAS), neutron activation analysis, X-ray fluorescence spectrometry, anodic stripping

voltammetry, atomic fluorescence spectrometry (AFS), and ion-selective membrane electrodes have been exploited for the sensing of nickel in environment samples [7–12]. However, these instrumentation techniques have various disadvantages like as expensive and sophisticated operating process, some basic interference, sample bounded adaptability, obligation of instrumentation experts, and time consuming methods. Recently, the optical sensing is high significant research area in analytical chemistry with advanced and simple techniques, owing to operational simplicity, high selectivity, cost effectiveness, high sensitivity, rapid process, direct visual perception, and high utility in human and biological research.

To date, many chemosensors have been investigated, and it has been widely demonstrated based on coumarin, anthracene, fluorophore [13–19], these reported sensors have limited choice due to complicated mechanism and supramolecular assemblies.

We have an ongoing interest to design and synthesis of simple small molecular sensor with low cost [20–27]. Herein, develop a simple, facile and reliable Ni<sup>2+</sup> fluorescent chemosensor based on a new thiazole derivative compound (**M1**) with an C=N and –OH linkage. Addition of methanolic solution of Ni<sup>2+</sup> to **M1**, exhibited a rapid blue shift in fluorescence emission spectra from 460 to 378 nm. Furthermore, electrochemical sensing studies of chemosensor **M1** to Ni(II) ions are also examined on DPV. These sensing phenomena consent it for high selective naked eye sensor for Ni<sup>2+</sup> ion over a various number of competitive ions such as alkali, alkaline, rare earth, and transition metal ions.

## 2. EXPERIMENT

### 2.1. Chemicals and instruments

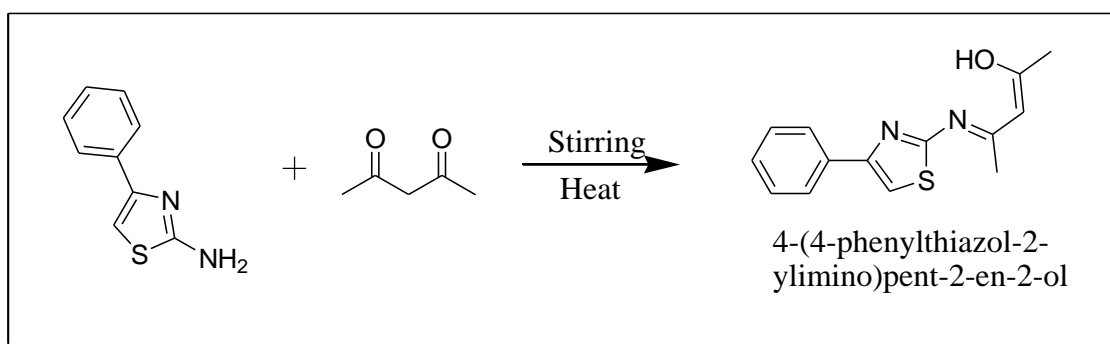
Reactants pentane-2,4-dione and 2-amino-4-phenylthiazole were used without further purification. Chloride and nitrate salt of all cations were used (Merck and Aldrich) with high purity and without further purification.

Nuclear magnetic resonance spectra (<sup>1</sup>H and <sup>13</sup>C) of chemosensor were recorded on Bruker Avance 500 (USA) with using CDCl<sub>3</sub> as a solvent using TMS as an internal standard. The FT-IR spectra were obtained on Nicolet 6700 FT-IR spectrometer with KBr pellets in the range 4000–400 cm<sup>-1</sup>. The absorption and fluorescence emission spectra were recorded using Shimadzu UV-2450 spectrophotometer and Shimadzu RF-5301 PC spectro-fluorophotometer (Japan), respectively, with quartz cuvette (path length = 1 cm). All pH studies on sensor were measured with Eutech pH-510. All experimental recognition between compound (**M1**) and various metal cations were explored with absorbance and fluorescence spectroscopy in methanol solution. The stock solution of **M1** and various metal ions (1.0 × 10<sup>-3</sup> M) were prepared in methanol. All emission spectral studies were carried out with excitation and emission slit width at 5.0 nm. Electrochemical sensing studies were examined on CHI760E electrochemical workstation (USA).

### 2.2. Synthesis of ionophore **M1**:

4-(4-phenylthiazole-2-ylimino)pent-2-en-2-ol (**M1**) was synthesized accordingly scheme-1 [28]. 10 mmol Pentane-2,4-dione (1.00 g) and 10 mmol of 2-amino-4-phenylthiazole (1.76 g) were

mixed and vigorously stirred for 2 hours and poured into 15 mL cold ethanol. After cooling, the yellowish crystalline product was obtained. (Yield 40%),  $^1\text{H}$  NMR spectrum (in  $\text{CDCl}_3$ ),  $\delta$ , ppm: 13.24 (s, -OH), 7.75 (d, 1H), 7.31 (t, 2H), 7.21 - 7.29 (m, 2H), 6.95 (s, H), 5.24 (s, 1H), 2.42 (s, 3H), 2.06 (s, 3H).  $^{13}\text{C}$  NMR spectrum (in  $\text{CDCl}_3$ ),  $\delta$ , ppm: 160.59, 156.89, 152.11, 134.11, 128.53, 127.95, 125.92, 105.98, 101.10, 99.99, 29.53, 29.23. Found, %: C 65.09, H 5.46, N 10.84, S 12.42.  $\text{C}_{16}\text{H}_{12}\text{N}_2\text{OS}$ . Calculated, %: C 64.98; H 5.31, N 10.69; S 12.61 [Fig. 1, 2]



**Scheme 1.** Synthetic Pathways of M1.

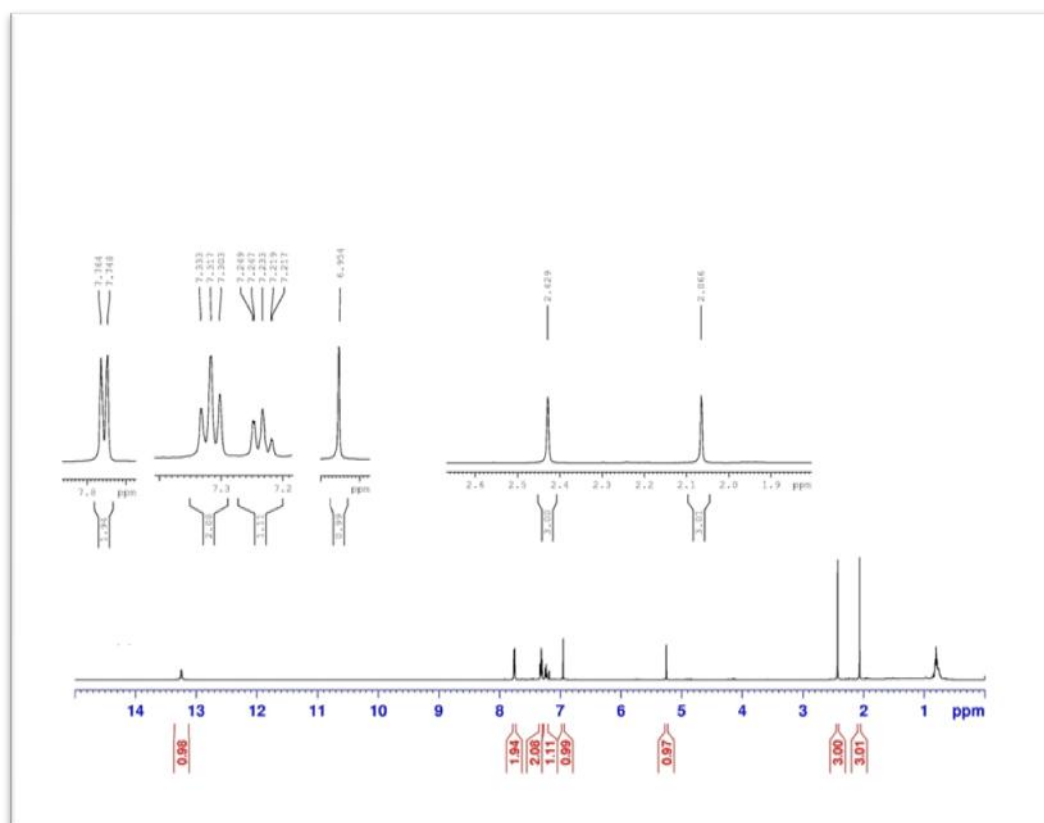


**Figure 1.**  $^1\text{H}$  NMR spectra of receptor M1.

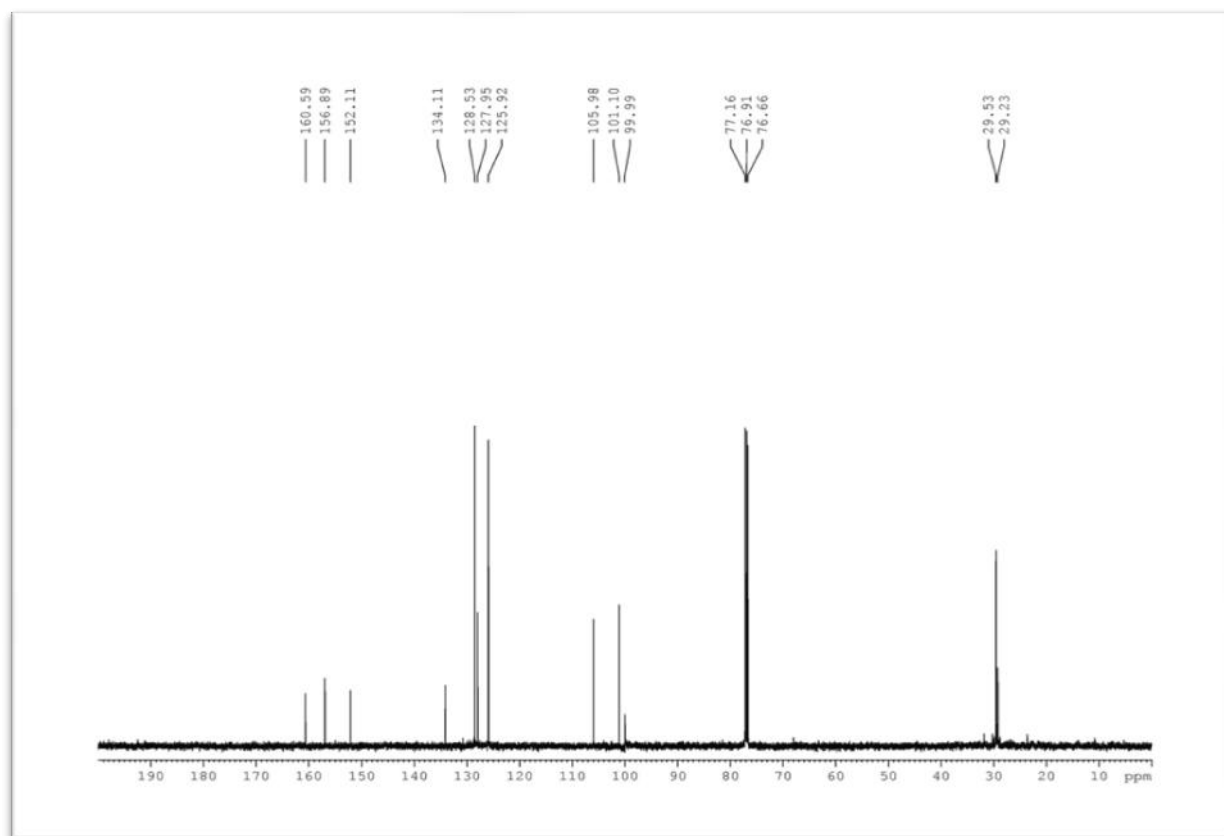


**Figure 2.**  $^{13}\text{C}$  NMR spectra of receptor M1.

### 3. RESULTS AND DISCUSSION

#### 3.1. The design of chemosensor **M1**

4-(4-phenylthiazole-2-ylimino)pent-2-en-2-ol (**M1**) with linked by C=N and –OH bond are selected as a potentially selective sensing molecule for the detecting metal ions. It is known that C=N, –OH (chelating groups) showed a high binding affinity towards transition and post-transition metal ions comparatively to alkali, alkaline and rare earth metal ions. Therefore, we constructed compound **M1** as fluorescent chemosensor. Firstly, 4-(4-phenylthiazole-2-ylimino)pent-2-en-2-ol was synthesized by reacting pentane-2,4-dione with 2-amino-4-phenylthiazole *via* single-step condensation reaction as shown in Scheme 1 and characterized *via*  $^1\text{H}$  NMR,  $^{13}\text{C}$  NMR and elemental analysis.

#### 3.2. Fluorescence studies of receptor **M1**

To investigate sensing properties of the receptor **M1** (40 ppm) towards various metal ions like as  $\text{Al}^{3+}$ ,  $\text{Mn}^{2+}$ ,  $\text{Cd}^{2+}$ ,  $\text{Ag}^+$ ,  $\text{Co}^{2+}$ ,  $\text{Fe}^{3+}$ ,  $\text{Ca}^{2+}$ ,  $\text{Cr}^{3+}$ ,  $\text{Cu}^{2+}$ ,  $\text{K}^+$ ,  $\text{Hg}^{2+}$ ,  $\text{Mg}^{2+}$ ,  $\text{Ni}^{2+}$ ,  $\text{Na}^+$ ,  $\text{Gd}^{3+}$ ,  $\text{Pb}^{2+}$  and  $\text{Zn}^{2+}$  were examined (Fig. 3). Receptor **M1** exhibited maximum fluorescence intensity at 460 nm, after the addition of various metal ions (except of  $\text{Ni}^{2+}$ ) fluorescence intensity remaining unchanged at 460 nm. In the presence of  $\text{Ni}(\text{II})$  ions maximum fluorescence peak dramatically shifted to lower wavelength

from 460 nm to 378 nm with 2 equivalent intensity enhancement provided optical information about the new complex formation in between the receptor M1 and  $\text{Ni}^{2+}$ .

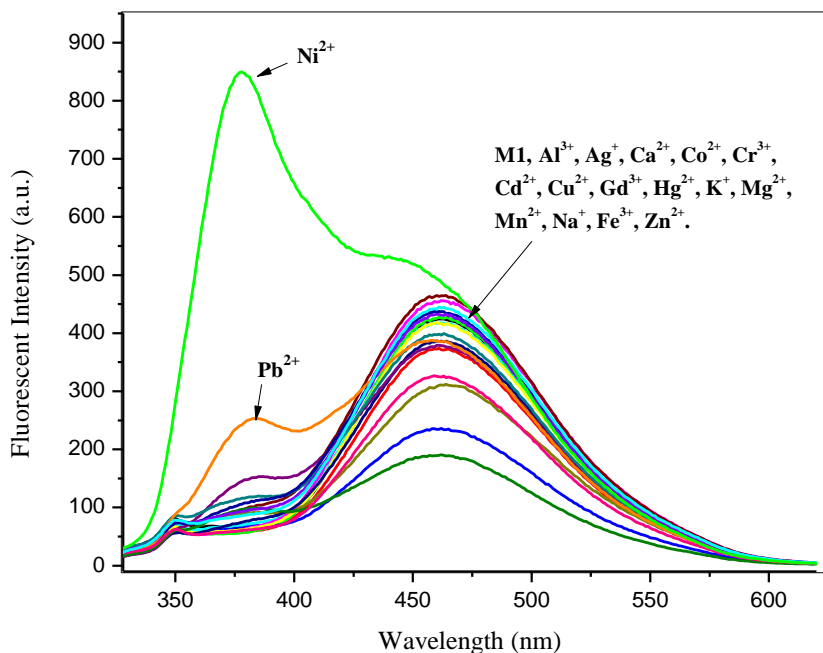


**Figure 3.** Emission spectra for the sensor M1 (40  $\mu\text{M}$ ) in the absence and presence of 1 equiv. of various metal ions, such as  $\text{Al}^{3+}$ ,  $\text{Cd}^{2+}$ ,  $\text{Ag}^+$ ,  $\text{Co}^{2+}$ ,  $\text{Ca}^{2+}$ ,  $\text{Cr}^{3+}$ ,  $\text{Fe}^{3+}$ ,  $\text{Mn}^{2+}$ ,  $\text{Hg}^{2+}$ ,  $\text{Na}^+$ ,  $\text{Cu}^{2+}$ ,  $\text{K}^+$ ,  $\text{Gd}^{3+}$ ,  $\text{Pb}^{2+}$ ,  $\text{Ni}^{2+}$ ,  $\text{Mg}^{2+}$  and  $\text{Zn}^{2+}$  in MeOH.

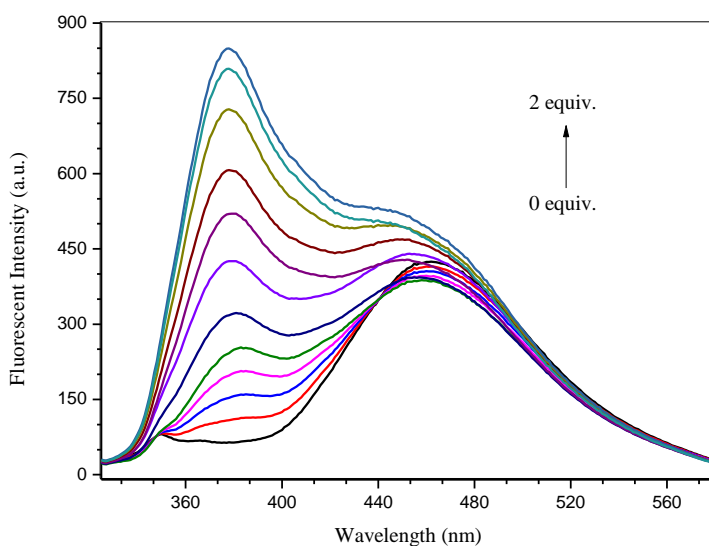


**Figure 4.** Fluorescence spectrum changes of sensor M1 (40  $\mu\text{M}$ ) with increasing concentration of  $\text{Ni}^{2+}$  (0, 3, 6, 9, 12, 15, 20, 25, 30, 35, 40, 80  $\mu\text{M}$ ) at  $\lambda_{\text{max}}$  of 378 nm.

Furthermore quantitatively evaluate, titration studies between fluorescence receptor and Ni(II) ions were examined in variable concentrations of Ni<sup>2+</sup> ions on fluorescence spectroscopy. Upon increasing the concentration of Ni<sup>2+</sup> ions (0.0 equivalents to 2.0 equivalents), fluorescence emission intensity enhanced gradually at maximum wavelength (378 nm). As visualized in Fig. 4, photofluorescence intensity at maxima enhanced with a linear range (R<sup>2</sup> = 99.2).

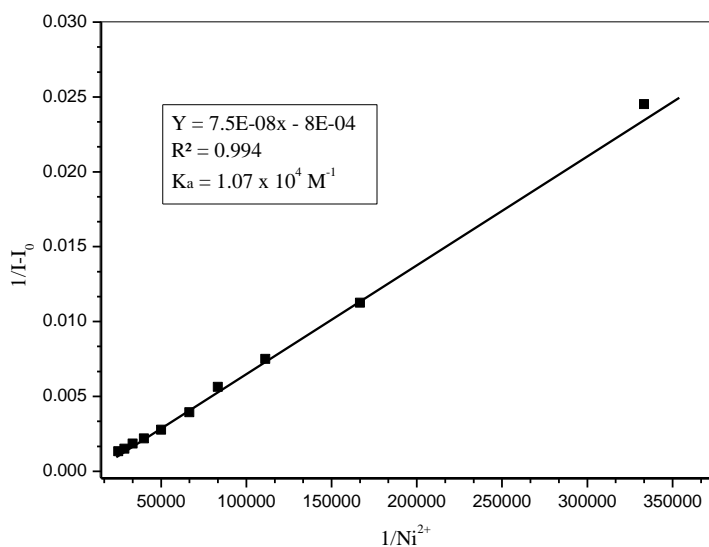


**Figure 5.** Benesi–Hildebrand plot for chemosensor M1 and Ni<sup>2+</sup> (maximum fluorescence intensity at 378 nm).

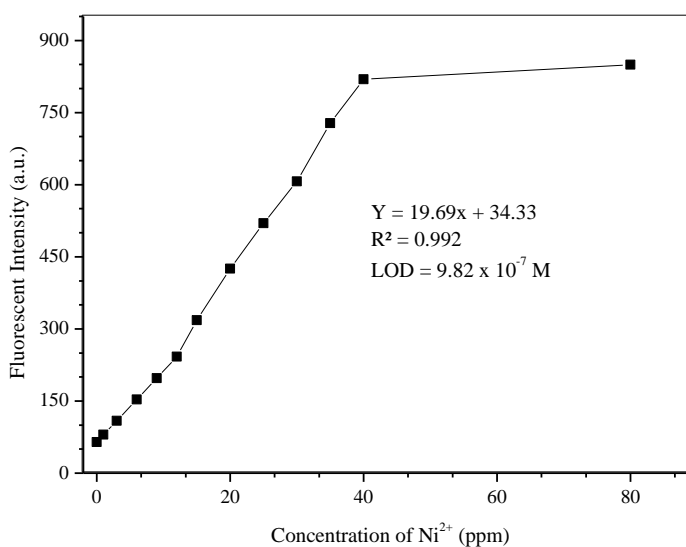


**Figure 6.** The linear relation for fluorescent intensity of M1 (40 μM) toward Ni<sup>2+</sup> concentration in the range of 0-40 μM.

The notable binding constant for respective complexes ( $M1+Ni^{2+}$ ) was examined with the help of Benesi–Hildebrand (B–H) plot [29]. The binding constant for  $M1+Ni^{2+}$  complex were calculated by slope of the linear plot and obtained  $1.07 \times 10^4 M^{-1}$  (Fig. 5).

Moreover, the detection limit of M1 for  $Ni^{2+}$  was calculated  $9.82 \times 10^{-7} M$  (Fig. 6) with the standard blank measurement ( $3\sigma/\text{slope}$ ) and gains the slope by concentration titration [30].

### 3.2. Selectivity of chemosensor **M1**

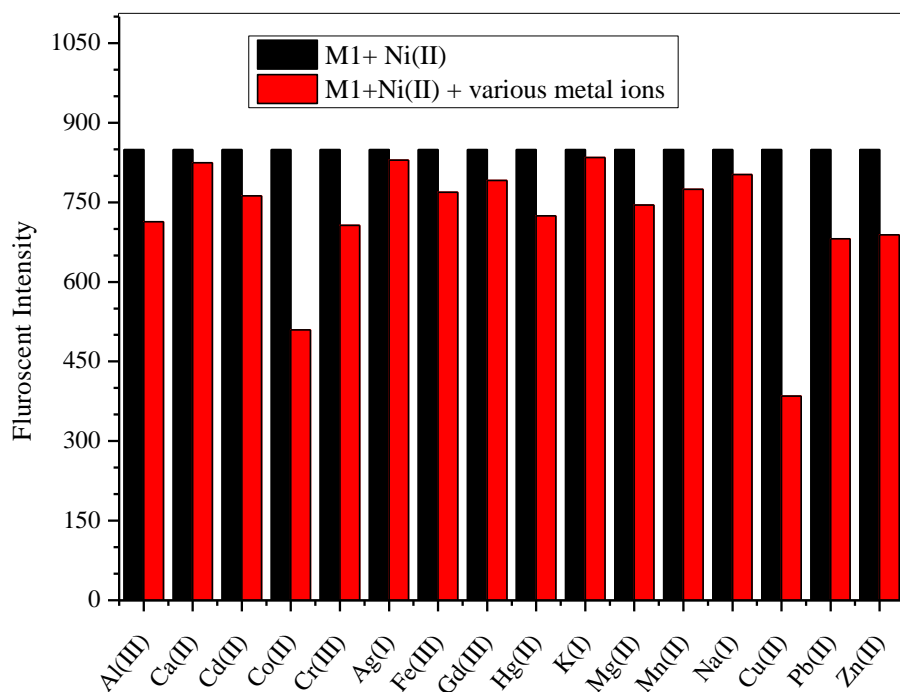
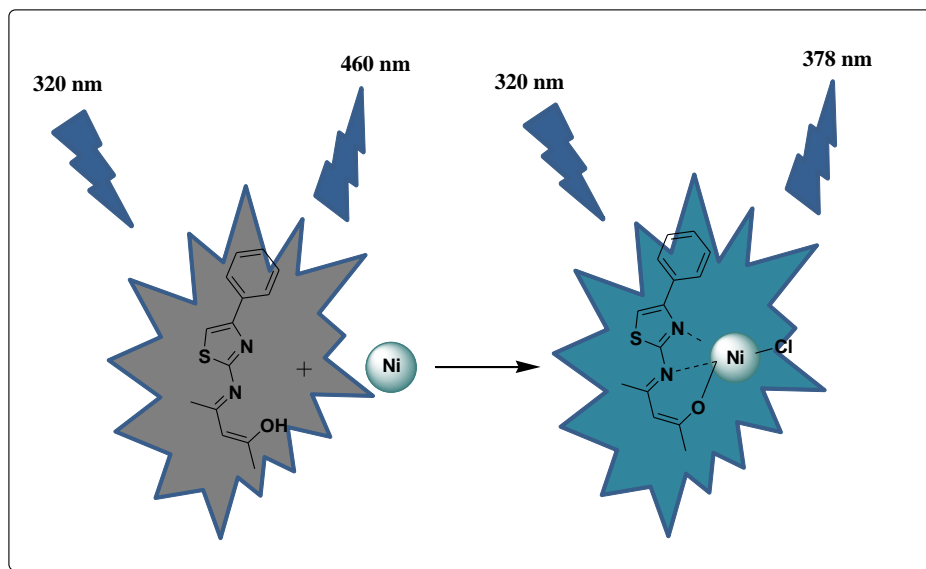


**Figure 7.** Interferences from different metal ions to the spectrophotofluorometric determination of  $Ni^{2+}$  ion for M1.

The influence of other competing metal ions on the fluorescence sensing of  $Ni^{2+}$  was also evaluated (Fig. 7). The fluorescence of M1 with metal ions  $Al^{3+}$ ,  $Cd^{2+}$ ,  $Ag^+$ ,  $Co^{2+}$ ,  $Ca^{2+}$ ,  $Cr^{3+}$ ,  $Fe^{3+}$ ,  $Mn^{2+}$ ,  $Hg^{2+}$ ,  $Na^+$ ,  $Cu^{2+}$ ,  $K^+$ ,  $Gd^{3+}$ ,  $Mg^{2+}$ ,  $Pb^{2+}$  and  $Zn^{2+}$  could not be red shifted or highly quenched, indicating that high selective fluorescence sensing of **M1** toward  $Ni^{2+}$  ions was insignificantly disturbed through competing metal ions except  $Cu^{2+}$  and  $Co^{2+}$ . The receptor **M1** response for  $Ni^{2+}$  in the presence of  $Cu^{2+}$  and  $Co^{2+}$  are relatively low but clearly detectable. This distinct selectivity for  $Ni^{2+}$  ions is probably achieved due to several factors, such as the suitable conformation of ligand and the ionic radius of the Nickel. Thus, the chemosensor M1 could be utilized as a significant fluorescent chemosensor for  $Ni^{2+}$  ions in the existence of competing cations (scheme 2).



**Scheme 2.** The proposed fluorescence sensing mechanism of chemosensor M1 towards Ni<sup>2+</sup> ions.

### 3.3. Job's plot analyse

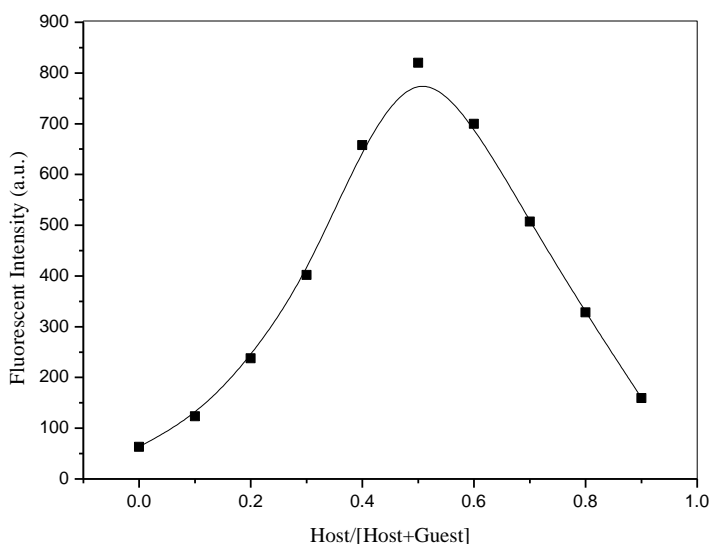


**Fig. 8.** Job's plot spectra for chemosensor M1 and Ni<sup>2+</sup> (maximum fluorescence intensity at 378 nm).

Forever, the stoichiometry of **M1**+Ni<sup>2+</sup> complex was examined through Job's plot method. In this method, the total concentration of **M1** and Ni<sup>2+</sup> (40.0 μM) keeping constant, and variable the molar ratio of Ni<sup>2+</sup> ([Ni<sup>2+</sup>]/[**M1** + Ni<sup>2+</sup>]) from 0.1 to 0.9. As shown in Fig. 8, the fluorescence emission got maximum at 0.5 molar fraction of Ni<sup>2+</sup>, indicating that **M1** and Ni<sup>2+</sup> forming a 1:1 complex.



### 3.4. Reversible sensing

The reversible sensing nature of chemosensor is an important aspect of sensing phenomena.

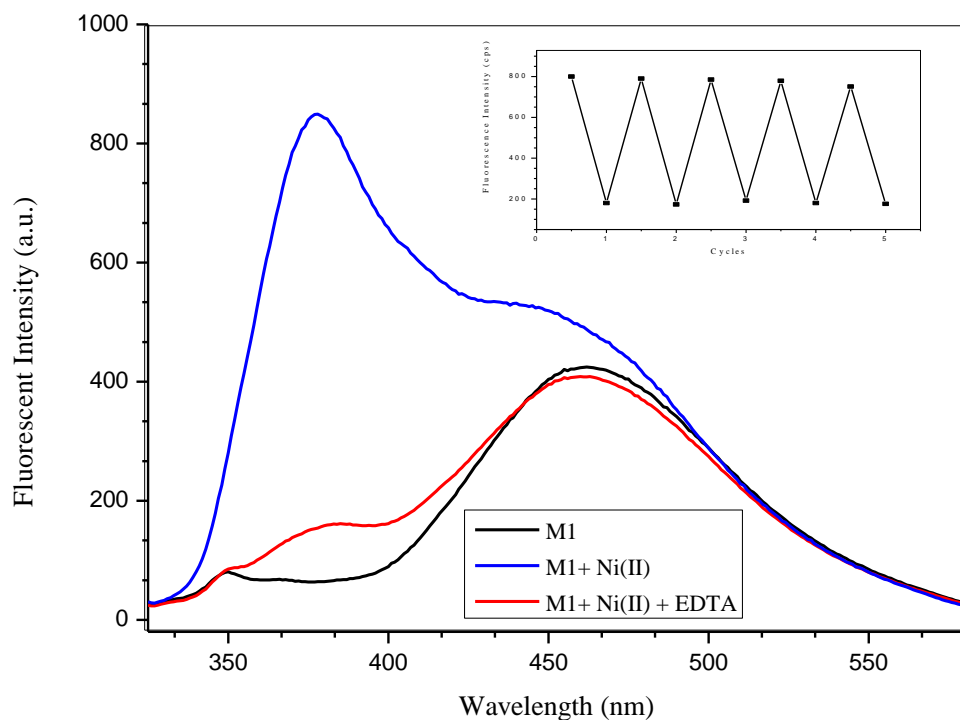


**Figure 9.** Reversible fluorescence intensity of **M1** (40  $\mu\text{M}$ ) at 378 nm upon alternate addition of a constant amount of  $\text{Ni}^{2+}$  (1 equiv.) and Inset: alternate signal of fluorescence reversibility.

As shown in Fig. 9, after the addition of EDTA, fluorescence emission intensity declined to lower level for chemosensor **M1** at 378 nm. Similarly as shown in Fig. 14 (inset), the alternate additions of a constant amount of  $\text{Ni}^{2+}$  and EDTA to the solution of **M1** exhibited a switchable change in the fluorescence intensity at 378 nm. Such reversible fluorescence behavior of **M1** can be repeated several times.

### 3.5. Electrochemical measurement of **M1**.

Chemosensor **M1** exhibited dual sensing (optical and electrochemical) signals for  $\text{Ni(II)}$  ion. Chemosensor **M1** in methanol was explored some notable changes in electrochemical signal in the existence of  $\text{Ni(II)}$  ions as visualized in Fig. 10. Oxidation potential for **M1** and **M1**+ $\text{Ni(II)}$  were recorded at 0.491, 1.003 V and 0.685, 1.159 V, respectively. The oxidation potential value for **M1**+ $\text{Ni(II)}$  shifted to more positive voltage compare the **M1**. These notable potential changes were exhibited the formation of complex between the probes **M1** and  $\text{Ni(II)}$  metal ions.

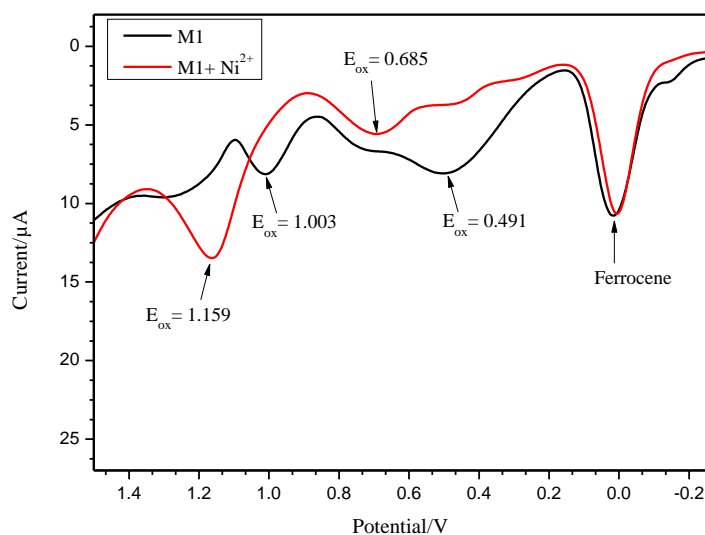


**Figure 10.** Electrochemical sensing studies of **M1** with Ni(II).

### 3.6. pH effect

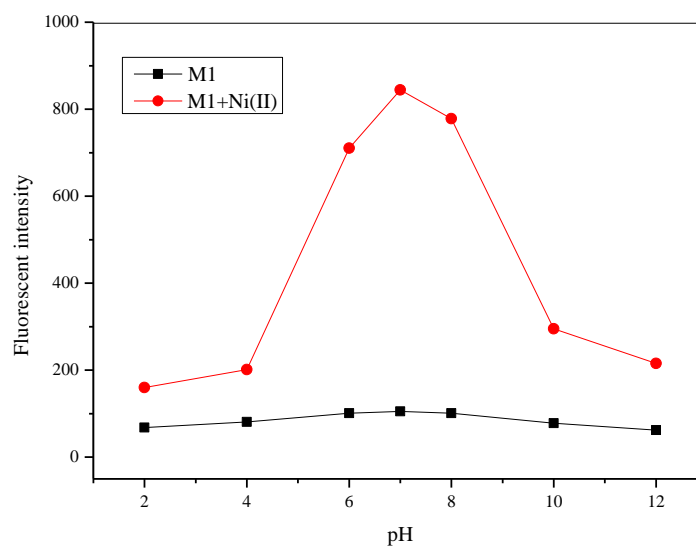


**Figure 11.** fluorescence emission (at  $\lambda_{\max} = 378$  nm) spectral changes of **M1** and **M1-Ni<sup>2+</sup>** complex with pH variations.

The effect of pH on the fluorescence sensing response of chemosensor towards Ni<sup>2+</sup> was investigated in MeOH. The fluorescence emission intensities of **M1** in the presence and absence of Ni<sup>2+</sup> were recorded at variable pH range (2.0–12.0). As shown in Fig. 11, receptor **M1** and its complex did not produce any characteristic fluorescence in acidic pH range (2.0–5.0) and weak fluorescence in basic medium (9.0–12.0 pH), the best sensing response was obtained only in 6–8 pH range.

## 3.6. Compare with previously reported sensor

**Table 1.** A comparative studies of reported probes with other sensor.

Ref.	Binding Constant ( $M^{-1}$ )	Detection Limit (M)	Response time	Interfering ions
32	$2.34 \times 10^4$	$5.0 \times 10^{-7}$	Turn-On	Co(II)
17	$4.50 \times 10^3$	-	Turn-On	Cu(II), Hg(II)
31	$2.20 \times 10^5$	$1.5 \times 10^{-7}$	membrane	-
12	-	$1.67 \times 10^{-6}$	Turn-off	Co(II)
15	$1.50 \times 10^4$	$5.0 \times 10^{-6}$	Turn-On	Cu(II)
18	-	$1.0 \times 10^{-6}$	Turn-On	Cu(II)
Probe M1	$1.07 \times 10^4$	$9.8 \times 10^{-7}$	Turn-on	No

A comparative studies of reported probes M1 with previously reported ion selective and fluorescence sensor on the Ni(II) ions in terms of their response time, binding constant, sensing ions, limit of detection, and selectivity towards Ni(II) ions in the appearance of interfering ions. The comparative result were shown in table-1, the reported sensor has good position [51-58].

## 4. CONCLUSION

In summary, here designed and synthesized a simple highly selective and sensitive electrochemical and fluorescent chemosensor based on thiazole derivative groups. The receptor M1 exhibited dramatic ratiometric fluorescence selectivity for  $Ni^{2+}$  ions over other competitive metal ions. More importantly, the chemosensor M1 was sufficiently low to detect 0.1 ppm concentrations of  $Ni^{2+}$ . The effective 1:1 stoichiometry coordination ability of  $Ni^{2+}$  metal ions with M1 was supported by high binding constants and job's method. Results were exhibited that reported sensors could be considered as a highly sensitive, selective, easy and cost-effective fluorometric method for the routine analysis of  $Ni^{2+}$ .

## ACKNOWLEDGEMENTS

Author is thankful to UGC and DST, Govt. of India, for the financial support.

## References

1. B. Bodenant, T. Weil, M.B. Pourcel, F. Fages, B. Barbe, I. Pianet and M. Laguerre, *J. Org. Chem.*, 64 (1999) 7034.

2. K.S. Kasprzak, A.A. Karaczyn, *J. Environ.l Monitor.*, 5 (2003) 183.
3. E. Denkhaus, K. Salnikow, *Crit. Rev. Oncol. Hematol.*, 42 (2002) 3.
4. F.W. Sunderman, L.M. Andersen, D. Ashley, F.A. Forouhar, *Ann. Cli. Lab. Sci.*, 19 (1989) 44.
5. N.W. Barnett, L.S. Chen, G.F. Kirkbright, *Anal. Chim. Acta*, 149 (1983) 115.
6. V.K. Gupta, R. Prasad, R. Mangla, P. Kumar, *Anal. Chim. Acta*, 420 (2000) 19.
7. K. Alizadeh, H. Nemati, S. Zohrevand, P. Hashemi, A. Kakanejadifard, M. Shamsipur, M.R. Ganjali, F. Faridbod, *Mater. Sci. Eng. C*, 33 (2013) 916.
8. M. Ghaedi, S.Y.S. Jaber, S. Hajati, M. Montazerzohori, M. Zarr, A. Asfaram, L.K. Kumawat, V.K. Gupta, *Electroanalysis*, 27 (2015) 1516.
9. S.L.C. Ferreira, W.N.L. dos Santos, V.A. Lemos, *Anal. Chim. Acta* 445 (2001) 145.
10. Z. Sun, P. Liang, Q. Ding, J. Cao, *J. Hazard. Mater. B*, 137 (2006) 943.
11. N. Yunes, S. Moyano, S. Cerutti, J.A. Gasquez, L.D. Martinez, *Talanta*, 59 (2003) 943.
12. H. Li, S.-J. Zhang, C.-L. Gong, Y.-F. Li, Y. Liang, Z.-G. Qi and S. Chen, *Analyst*, 138 (2013) 7090.
13. V.K. Gupta, N. Mergu, A.K. Singh, *Sens. Actuators B*, 220 (2015) 420.
14. A.P. de Silva, H.Q.N. Gunaratne, T. Gunnlaugsson, A.J.M. Huxley, C.P. McCoy, J.T. 275 Rademacher, T.E. Rice, *Chem. Rev.*, 97 (1997) 1515.
15. N. Chattopadhyay, A. Mallick, S. Sengupta, *J. Photochem. Photobio.*, 177 (2006) 55
16. V.K. Gupta, A.K. Singh, L.K. Kumawat, *Sens. Actuators B*, 195 (2014) 98.
17. Fasil A. Abebe, Carla Sue Eribal, Guda Ramakrishna, Ekkehard Sinn, *Tetrahedron Lett.*, 52 (2011) 5554.
18. D.A. Pearce, G.K. Walkup, and B. Imperiali, *Bioorg. Med. Chem. Lett.*, 8 (1998) 1963.
19. S. Ghosh, R. Chakrabarty, P.S. Mukherjee, *Inorg. Chem.*, 48 (2009) 549.
20. V.K. Gupta, S.K. Shoor, L.K. Kumawat, A.K. Jain, *Sens. Actuators B*, 209 (2015) 15.
21. V.K. Gupta, A.K. Singh, N. Mergu, *Electrochim. Acta*, 117 (2014) 405.
22. L.K. Kumawat, N. Mergu, A.K. Singh, V.K. Gupta, *Sens. Actuators B*, 212 (2015) 389.
23. V.K. Gupta, A.K. Singh, L.K. Kumawat, *Sens. Actuators B*, 204 (2014) 507.
24. N. Mergu, V.K. Gupta, *Sens. Actuators B*, 210 (2015) 408.
25. V.K. Gupta, N. Mergu, A.K. Singh, *Sens. Actuators B*, 202 (2014) 674.
26. V.K. Gupta, N. Mergu, L.K. Kumawat, A.K. Singh, *Talanta*, 144 (2015) 80.
27. V.K. Gupta, A.K. Jain, S.K. Shoor, *Sens. Actuators B*, 219 (2015) 218.
28. S.E. Sadigova, A.M. Magerramov, M.A. Allakhverdiev, *Russ. J. Org. Chem.*, 44 (2008) 1848.
29. H.A. Benesi, J.H. Hildebrand, *J. Am. Chem. Soc.*, 71 (1949) 2703.
30. V.K. Gupta, N. Mergu, L.K. Kumawat, A.K. Singh, *Sens. Actuators B*, 207 (2015) 216.
31. M. Shamsipur, T. Poursaberi, A.R. Karami, M. Hosseini, A. Momeni, N. Alizadeh, M. Yousefi, M.R. Ganjali, *Anal. Chim. Acta*, 501 (2004) 55.
32. J. Jiang, C. Gou, J. Luo, C. Yi, X. Liu, *Inorg. Chem. Commun.*, 15 (2012) 12.